Landward mantle flow associated with the Pacific subduction system opened the South China Sea

Yanhui Suo (suoyh@ouc.edu.cn)
Ocean University of China
Hao Dong
Ocean university of China https://orcid.org/0000-0002-7620-0266
Lijun Liu
University of Illinois at Urbana Champaign
Diandian Peng
University of Illinois at Urbana-Champaign https://orcid.org/0000-0002-8664-2164
Yanchong Li
University of Illinois at Urbana-Champaign https://orcid.org/0000-0002-9075-3887
Jinping Liu
Ocean University of China
Liming Dai
Ocean university of China
Xianzhi Cao
Ocean University of China
Sanzhong Li
Ocean University of China

Article

Keywords:

Posted Date: December 19th, 2022

DOI: https://doi.org/10.21203/rs.3.rs-2332418/v1

Abstract

Whether Tethyan or Pacific subduction controlled the formation of the South China Sea (SCS) is debated. Here, using high resolution seismic data, we reveal that the continental extension across the northern SCS margin experienced a transition from the Early-Eocene narrow-rift mode to the Late Eocene wide-rift mode. Using 4D geodynamic models, we propose that the evolving rifting mode was dominated by the landward mantle flow associated with Pacific subduction: 1) Toroidal mantle flow through a hole in the retreating flat slab initially thinned the continent to form a narrow rift; 2) Strong landward mantle wind through a broad trench-parallel slab window since ~40 Ma stretched the narrow rift into a wide rift and eventually an oceanic basin. We conclude that the landward mantle flow represents a new mechanism of continental extension, where increasingly strong hot upwelling caused the intermediate SCS rifted margin between the traditional magma-poor and magma-rich end-members.

Introduction

South China Sea (SCS) formed in a unique tectonic context, where the Indo-Australian, Eurasian, (Paleo-) Pacific, and Philippine Sea plates formed a super-convergence tectonic regime[1] since the Gondwana dispersion (Fig. 1). Multiple lines of geological evidence involving volcanic arcs, ophiolites, accretionary complexes, and marginal basins reveal the existence of ancient oceans in this region, i.e., the Paleo-Tethys, Neo-Tethys, Paleo-Pacific, and Pacific. Therefore, the SCS is a natural laboratory to study the dynamic interactions between the Tethyan and Pacific tectonic domains.

Despite that multiple conceptual 2D models have tried to connect the Tethyan and Pacific tectonic domains[2-4], whether the Tethyan tectonic domain or the Pacific tectonic domain dominated the development of the SCS has long been a matter of debate due to the complex subduction system. It sparked two controversial issues around the SCS region: 1) the rifting process of the ultra-wide (up to 1000 km) northern SCS passive margin is different from extension styles in typical Atlantic passive margins or East Asian back-arc regions, by challenging the typical magma-poor and magma-rich end-members with combined features of both[5-8]. 2) The abrupt opening of the SCS has invoked a variety of proposed models, e.g., back-arc extension model[9], extrusion model of the Indochina Peninsula[10-11], proto-SCS (PSCS) dragging model[12-14], mantle plume intrusion model[15] and plate-edge rifting model[16]. In addition, deep-mantle constraints from seismic tomography and azimuthal anisotropy further complicate the situation, such as the presence of various types of mantle flow in the Celebes Basin[17] and the northward dipping PSCS slab[18-19]. Thus, 4D (space and time) mantle convection modelling is a key approach to unraveling the geodynamic history and the mechanism in the formation of the SCS.

The Pearl River Mouth Basin (PRMB) is the largest Cenozoic rift basin on the northern SCS margin (Fig. 1). Industry wells and seismic data throughout the PRMB[20-23] indicate it well records the transition from continental rifting to continental breakup and the subsequently rapid onset of seafloor spreading[24]. Here, using high resolution seismic data, we imaged the crustal structure of the western

PRMB. Then, using 4D global geodynamic models assimilating constraints from plate reconstructions[25-26] (Fig. S1), we reproduced the Mesozoic-Cenozoic subduction history. This work allowed us to examine the spatial-temporal correlation between lithospheric deformation and mantle dynamics in the overall convergent context of the Tethyan and Pacific tectonic domains. Our geodynamic models predicting the landward mantle flow associated with Pacific subduction reveal a new mechanism of continental extension in the entire East Asian margin, which contrasts the typical passive margins or back-arc regions. The enduring landward mantle flow allowed increasing amounts of hot upwelling that weakened and rifted the intermediate SCS margin. Some other forces around the SCS region contributed to facilitating the transition from continental rifting to breakup that opened the SCS abruptly at 32 Ma, when other East Asian active margins were still in the rifting phase.

Observed Scs Crustal Structure

Syn-rift crustal structure. The seismic data (Fig. 1) cover the Enping Sag in the proximal domain, the Baiyun Sag in the necking domain, and the Liwan Sag in the distal domain[27]. A set of first-order interfaces are interpreted as: Tg, T80 and T70 (Figs. 2a-b). Tg corresponds to a regional unconformity between the pre-Cenozoic and Cenozoic throughout the whole SCS area. It shapes the basement configuration and represents the diachronous continental rifting initiated from 60 Ma to ~49 Ma. T80 represents a basin-wide unconformity at ~39 Ma. T70 terminates with onlapping geometry toward Tg, marking the cease of continental rifting at ~32 Ma. Separated by T80, the syn-rift sequence (Tg–T70) in the PRMB is composed of two units: the lower Eocene syn-rift unit and the upper Eocene syn-rift unit[27-28].

The lower Eocene syn-rift unit is filled with the Wenchang Formation (Tg–T80). Controlled by normal faults limited at the brittle upper crust level, the geometry of the Wenchang Formation was divided into a series of symmetric grabens (Figs. 2a-b). In plain view, each graben extends over a short distance (<100 km) along ENE-striking and the region of intense normal faulting is locally concentrated (Fig. 2c). The crustal stretching factor was estimated to be 1.2[29], no larger than the thickness of the continental lithosphere. The symmetric sag geometry and the localized normal faults within the weak stretched crust imply that the Early Eocene continental extension results in a narrow rift in the PRMB (Fig. 2c), a dominant mode of the conventional rifting that has also been observed in the Baikal Rift and the East African Rift System[30-31].

The upper Eocene syn-rift unit is filled with the wedge-shaped Enping Formation (T80–T70), mainly controlled by the seaward dipping boundary faults (Figs. 2a-b). They evolved into the detachment faults in the Baiyun Sag and Liwan Sag, which penetrated deep into the lower crust and exhibited ductile deformation. Sub-parallel to the Liwan detachment fault, an isocline of seismic energy was organized into a pattern documenting 30–40 km long nappe folds[23] or mega-sheath folds[32] (Figs. 2a-b). The dome or boudinage structure that are common onshore South China were also delineated within the lower crust, constituted by the ENE-striking nappe thrusts and the NE-striking transpressional faults[27] (Figs. 2a-b). The interior of the wedge-shaped Enping Formation were overprinted by another group of steeply dipping

faults. In plain view, these steep faults extend over a long distance in right-lateral *en échelon* arrangement along NE-striking, serving as the long side of a rhomb-shaped pull-apart basin. Meanwhile, the boundaries or detachment faults of each sag act as the ENE-trending short side of this rhomb-shaped pull-apart basin (Fig. 2d). The crustal stretching factor during this syn-rift phase was estimated to be ~3[29], with cumulative extension three times the thickness of the continental lithosphere. The asymmetric sag geometry and the highly extended continent imply that the narrow rift had transited into the wide rift[7] (another dominant mode of the conventional rifting) during the Late Eocene syn-rift phase (Fig. 2d), similar to the broad rifts in the Basin & Range province in western United States and in the Aegean Sea[30].

Post-rift crustal structure. The continental rifting ceased in the distal domain and the PRMB entered the post-rift phase after ~32 Ma[12, 14], marked by the commencement of the E-W-striking or ENE-striking spreading center in northeastern SCS[7, 33]. The spreading center in northeastern SCS jumped southward at ~23.6 Ma and became extinct until 15 Ma[34], forming the East Subbasin with a wide-open side on the east. Contemporarily, the seafloor spreading propagated to the west and ceased at 16 Ma, forming the triangle-shaped Southwest Subbasin[33, 35] (Fig. 1).

Modeled Subduction Structure And Mantle Flow

We performed two high-resolution global geodynamic models (Fig. S2) with data-assimilation since 200 Ma: Model 1 used the plate reconstruction from ref.[26] as time-dependent boundary conditions and Model 2 used the plate reconstruction from ref.[25]. The major differences between the two plate reconstructions (Fig. S1) were summarized in the supporting information. Model setup and parameters followed recent studies[36–38], and the detailed information could be found in Method.

Model 1 is our preferred model. In the upper mantle, the geometry of the predicted present Pacific slab and SCS slab (Fig. 3a) show a good match with high-velocity P wave anomalies in UU-P07[39] (Fig. 3c) and MITP08[40] (Fig. 3d). In the lower mantle, the large Neo-Tethyan and Izanagi slab piles (Fig. 3a) from the complex Tethyan and Pacific subduction are in general agreement with fast seismic anomalies (Figs. 3c-d). The broad flat Izanagi slab at the earliest Cenozoic (Fig. 4a) previously demonstrated in Ref.[41] is largely due to hydrodynamic suction from the long-lasting Mesozoic Western Pacific and Tethyan subduction, where progressively lowering dynamic pressure within the slabs-bounded upper mantle below East Asia led to flattening of the Izanagi slab during the Late Cretaceous. By 60 Ma, this flat slab started to detach from the base of the overriding lithosphere along most of the East Asian margin[36] (Fig. 3a), with a prominent slab hole developed in the study area (Fig. 4a and Fig. S2a), largely along a NW-striking transform plate boundary between the fossilized PSCS and (Paleo-) Pacific plates (Fig. S1a). Through this slab hole, the hot asthenosphere below the Izanagi and Pacific plates flowed into the mantle wedge under South China, forming a clockwise toroidal mantle flow (Fig. 4a). This flow pattern is similar to that below the Basin & Range province in western United States, following the segmentation of the Farallon slab[42], thus representing a novel mechanism for the extension of the overriding South China lithosphere[43].

By ~ 40 Ma, the slab hole grew into a broad trench-parallel slab window under the entire East Asian margin (Fig. 4b and Fig. S2a), due to the trench-parallel subduction of the Izanagi-Pacific mid-ocean ridge[36]. The broad slab window provided a pathway that connected the mantle wedge beneath East Asia with the approaching asthenosphere below the Pacific Plate, giving rise to the strong landward mantle wind[38] (Figs. 3a and 4b) and basal traction[36]. Contemporaneously, the Philippine Sea Plate (PSP) began to occupy the region to the east of the PSCS since ~ 40 Ma (Fig. S1a). The clockwise rotation of the PSP resulted in a sinistrally strike-slip motion along the NW-striking transform plate boundary[44]. Through the open door along the transform plate boundary, the hot asthenosphere under the young PSP also flowed northwestward, endeavoring to be a component of the landward mantle wind (Fig. 4b and Fig. S2a). The mantle wind exerted a strong landward basal traction and profoundly thinned the overriding lithosphere to the east of the North-South Gravity Lineament[45], along which a boundary separating the Pacific tectonic domain and Tethyan tectonic domain occurred (Fig. 4b). This boundary is predicted to extend into Southeast Asia, coinciding with the distribution of the Red-River Fault Zone and the West Baram-Tinjar Line[46] (Figs. 1 and 4b). As an important tectonic line between continental blocks that underwent differential extension in the Eocene[47], the Red-River Fault Zone and the West Baram-Tinjar Line also denotes an obstacle preventing the assembly of the mantle flows on both sides in our model (Fig. 4b). The mantle wind began to diminish since ~ 20 Ma, consistent with the widespread rifting termination in East Asian continental margin (i.e., the Bohai Bay Basin and the East China Sea Shelf Basin (ECSB)) that ceased by ~ 23 Ma[36, 48–49], as it was blocked by the subducting Pacific slab (Fig. 3a and Fig. S2a).

As shown above, the toroidal mantle flow through the slab hole and the subsequent mantle wind through the slab window (both are landward below East Asia) are likely responsible for the widespread East Asian continental extension[36]. To demonstrate that the formation of the landward mantle flow is robust under different plate reconstructions, we present Model 2 using the surface kinematics from ref.[25]. In Model 2, the present-day westward dipping slab under the Philippine Trench (Fig. 3b) shows an opposite subduction polarity with that observed in the two tomographic models (Figs. 3c-d), but other slab structures are similar. Model 2 recovers a similar dynamic history (Fig. 3b and Fig. S2b) as Model 1, both characterized by the prevalence of the mantle wind between ~ 40 Ma and ~ 20 Ma. However, prior to 40 Ma, Model 2 reproduces mostly a poloidal mantle flow pattern (Fig. 3b) due to assumed seafloor spreading within the PSCS. For this part of the SCS history, we prefer the toroidal flow pattern generated by the fossilized PSCS in Model 1, because abundant geological evidence revealed that the PSCS has a Mesozoic oceanic crustal age and has been subducted beneath Borneo during the Eocene and Early Miocene[12–13, 50–52]. Next, we examine the formation of this landward mantle flow to understand the rifting processes of the SCS margin.

Two-phase Continental Rifting Dominated By The Landward Mantle Flow

Role of the transform plate boundary. As seen in the two adopted plate reconstructions (Fig. S1), continental rifting of the PRMB was initiated along a passive margin where the PSCS was anchored to

South China (Fig. 5a). Contemporaneously, back-arc extension started[36, 47–48] along other East Asian margins where the subduction of the Izanagi Plate continued. In Model 1, a NW-trending transform plate boundary developed along the eastern boundary of the fossilized PSCS at the latest Cretaceous and the earliest Cenozoic[26]. The subducted flat Izanagi slab was transported by the lateral mantle flow (Fig. S2a) to the upper mantle southwest of this transform plate boundary below the PRMB (Figs. 3a and 5a). Therefore, we suggest the northward dipping fast anomaly below the present northern SCS region revealed by tomographic images[18–19] likely represents a piece of this displaced Izanagi slab[9, 53]. Accompanying the slab hole formed between the sinking slab and the transform boundary, the asthenosphere flowed into the mantle wedge under South China, resulting in the observed toroidal mantle flow (Figs. 4a and 5a). To the southwest of the transform boundary, the toroidal mantle flow pushed the overriding continental lithosphere northwestward (Fig. 5a). Meanwhile, the continental margin was trying to move away in the SE direction following trench retreat, offset by the sinsitral strike-slip movement along the transform plate boundary. These two motions in opposite directions stretched the overriding plate in the NW-SE direction, finally triggering the continental rifting and the formation of narrow rifts in the PRMB (Fig. 5a). To the northeast of the transform plate boundary, the toroidal mantle flow pushed the Izanagi slab to retreat, leading to back-arc extension and the formation of the ECSB in the overriding plate (Fig. 5a). Overall, the continental rifting in both the northern SCS passive margin and the East China Sea active margin were induced by the toroidal mantle flow around the slab edge between these two regions.

To illustrate the role of the toroidal mantle flow in dominating the continental rifting, we compared these results with those in Model 2. Model 2 generated a smooth and unfragmented flat slab at the same location as that in Model 1 prior to 40 Ma (Fig. S2), when the transform plate boundary in Model 1 was replaced by a subduction zone based on the adopted reconstruction in Ref.[25]. The broad flat slab usually induced lithospheric compression, as seen in the Laramide Orogeny[54], and was used to explain the earliest Cenozoic surface uplift and tectonic inversion in East Asian sedimentary basins[41]. Therefore, we proposed that the NW-trending transform plate boundary suggested in the new reconstruction of Ref.[26] is the key reason for the formation of the toroidal mantle flow and the resulting continental rifting. This NW-trending transform plate boundary was well recorded by the prominent NW-trending Yushan-Kume Fault Zone[55], which is located between the present PRMB and the ECSB (Figs. 1 and 5a). The Yushan-Kume Fault Zone was sinistrally strike-slipping at the latest Cretaceous[56], as it absorbed the large fractions of relative plate movement along the subducting transform plate boundary.

Role of the Izanagi-Pacific mid-ocean ridge. Through basal traction, the toroidal mantle flow in Model 1 dragged the buoyant Izanagi-Pacific mid-ocean ridge to continuously subduct westward[36]. The slab hole eventually grow into a broad trench-parallel slab window at ~ 40 Ma (Figs. 4b and 5b), associated with the complete subduction of the Izanagi-Pacific mid-ocean ridge under East Asia[36]. The broad trench-parallel slab window provided a pathway that connected the mantle wedge beneath South China with the approaching asthenosphere below the Pacific Plate, forming the strong landward mantle wind (Figs. 3a, 4b and 5b). The high-velocity mantle wind exerted a strong landward basal traction on the thick overriding continental lithosphere east of the North-South Gravity Lineament, stretching the narrow PRMB

rift into an asymmetric wide rift that is characterized by the highly extended crust and the seaward dipping detachment faults (Fig. 5b). Therefore, the trench-parallel subduction of the Izanagi-Pacific mid-ocean ridge is the key reason in forming the regional mantle wind and the resulting wide rift[36], which is also observed in Model 2 (Fig. 3b, Fig. 5b and Fig. S2b).

The slab hole and the subsequent slab window also allowed the occurrence of mantle upwelling and magmatism. The magmatism was weak during the narrow rifting phase (Fig. 5a), which was previously attributed to a strong or weak hot stretched lithosphere[57]. The volcanism ceased at ~ 50 Ma[58] as recorded in the northern SCS margin. The subsequent broad slab window during the wide rifting phase led to intense mantle upwelling (Fig. 5b), which could explain the 45–33 Ma magmatism along the northern SCS margin and even a pulse of the Hainan mantle plume[59–60]. The plume impingement in turn weakened the lithosphere, increased the lithospheric ductility and promoted the wide rifting to evolve into continental breakup and rapid onset of seafloor spreading as observed. The transition from narrow rift with weak magmatism to wide rift with intense magmatism along the northern SCS margin may represent an intermediate rifted margin between the magma-poor and the magma-rich end-members.

Involvement of pre-existing basement faults. As shown above, the landward mantle flow from the Pacific subduction system can explain the geodynamic discrepancies between two syn-rift phases in the northern SCS margin. In addition, the differences in structural architectures between the two syn-rift phases suggest the involvement of the pre-existing basement faults, which are common in rifted margins. The intra-basement boudinage structure (Figs. 2a-b), consisting of the ENE-striking thrusts and the NE-striking transpressional faults onshore-offshore the South China Block, have been delineated in the previous works[7, 27–28]. During the Early Eocene rifting, strains were mainly localized on the brittle upper crust and no basement structures were reactivated, leading to the formation of the ENE-striking short normal faults with a small crustal stretching factor of 1.2. During the Late Eocene rifting, lithospheric ductility was increased and strains migrated to the ductile lower crust, facilitated by the hot mantle upwelling through the broad slab window. So, the upper crustal ENE-striking normal faulting penetrated into the crystalline basement, resulting in the formation of the detachment faults and the reactivation of the pre-existing ENE-striking thrusts. Simultaneously, the pre-existing NE-striking transpressional faults were reversed into transtensional faults under the extension driven by the landward mantle wind. Reactivation of both the intrabasement ENE-striking and NE-striking faults led to the occurrence of the Late Eocene pull-apart basins *en échelon* (Fig. 2d), with a rhomb shape inherited from the pre-existing boudinage configuration.

Implications On The Opening Of The Scs

As seen in the geodynamic models, the landward mantle flow is a common phenomenon below the East Asian margin (Figs. 3a, 3b, 4b and Fig. S2). It generally lasted until ~ 20 Ma and is likely responsible for the widespread East Asian continental extension that ceased by ~ 23 Ma[36]. However, the northern SCS margin abruptly entered the seafloor spreading phase at ~ 32 Ma, when other East Asian margin regions

(i.e., the Bohai Bay Basin and the ECSB) were still in the rifting phase. It seems that, besides the landward mantle flow, some other forces around the SCS region further propelled the continental rifting into the seafloor spreading.

The extrusion of the Indochina Block[11, 61] and the PSCS dragging[13–14] are two popular models to explain the formation of the SCS. As proposed by the extrusion model, the India-Eurasia collision led to > 700 km southeastward extrusion of the Indochina Block along the left-lateral strike-slip Ailao Shan-Red River Fault[62–63] (Fig. 1). The strike-slip movement along the Ailao Shan-Red River Fault triggered the seafloor spreading and ridge jumps in the SCS. Consequently, the main force in the extrusion model should be concentrated along the western margin of the SCS, and this model cannot explain why the East Subbasin (33 – 15 Ma) formed earlier than the Southwest Subbasin (23.6–16 Ma). The PSCS dragging model suggested that the PSCS subducted under Borneo during ca. 34-15.5 Ma[64], coinciding with the seafloor spreading history of the SCS[46]. The southward-dipping subduction of the PSCS generated a slab pull that opened the SCS. However, this model is also questionable since paleomagnetic results show that the PSCS was very narrow and was unlikely to have pulled apart the thick continental lithosphere of South China[52].

Here, we emphasize the combined effects of the strike-slip faulting and the PSCS dragging [44, 65–66]. When the south-directed PSCS slab pull occurred at the earliest Oligocene, the extremely thin continent along the ENE-striking detachment faults was preferentially ruptured while the NE-striking transtensional faults still maintained the dextral strike-slip motion. So, oceanic spreading was firstly initiated along the ENE-striking faults with some lithospheric stretching being absorbed by the NE-trending strike-slip faults, similar to the pull-apart opening model of the Japan Sea[67–68]. Then the northeastern SCS ridge jumped southward at 23.6 Ma due to the acceleration of the PSCS south-directed subduction[66], though the extension scenario on the overriding plate induced by the landward mantle flow largely ended. The ongoing south-directed subduction of the PSCS drove the SCS spreading to last until ~ 16 Ma, when the PSCS was entirely consumed by the collision between Palawan and Borneo.

Although the PSCS dragging was probably involved in the spreading history of the SCS, it is the landward mantle flow associated with the Pacific subduction system that provided the essential and necessary extension condition for the onset of the SCS seafloor spreading. The PSCS dragging, whose direction is parallel to subduction zone on the east, may have facilitated the SCS opening. In contrast, the back-arc extension in the ECSB is directly against subduction zone on the east, which may have prevented the eventually continental breakup. The involvement of the PSCS dragging also distinguishes the ultra-wide northern SCS margin from the wide rifts in the Basin & Range province or the Aegean Sea, where continental breakup didn't occur. In conclusion, this work outlines a new mechanism of continental extension, which is different from extension in typical Atlantic passive margins or Western Pacific back-arc regions.

Data And Methods

Seismic interpretation. The crustal structure is mainly based on the interpretation of 3D seismic reflection lines, acquired by the China National Offshore Oil Corporation (CNOOC). The 3D seismic reflection data cover a total area of over 2.1 ×10^4 km^2, with a bin size of 20 × 20 m and a vertical resolution of ~ 20 m. The data recorded as deep as 11 s two-way travel time (TWTT).

The data-assimilation geodynamic model. We model 3-D spherical mantle flow with CitcomS code[69], which are widely used in simulating time-dependent mantle convection. Using plate velocities exported from plate reconstructions as boundary conditions, 4D global data-assimilation geodynamic models could reproduce the subduction history[42, 70]. The mantle was subdivided into 12 spherical caps each having 257 × 257 × 113 nodes in latitude × longitude × radius. The lateral resolution is ~20 km at the surface.

The Rayleigh number, which determines the vigor of mantle convection, is defined as

$$R_a = \frac{\alpha_0 \rho_0 g_0 \Delta T {h_M}^3}{\kappa_0 \eta_0}$$

1

Where α is the coefficient of thermal expansion, ρ is the density, g is the gravitational acceleration, ΔT is the temperature range between the earth's surface and the core-mantle boundary, h_M is the thickness of mantle, κ is the thermal diffusivity, and η is the viscosity. The subscript "0" represents the reference values.

The models incorporated a 3D viscosity structure that depends on depth, temperature and composition, calculated as follows:

$$\eta = \eta_0 (r) \exp\left(\frac{E_\eta}{R\left(T + T_\eta\right)} - \frac{E_\eta}{R\left(T_\mathrm{b} + T_\eta\right)}\right)$$

2

Where $\eta_0(r)$ is a depth-dependent pre-factor defined with respect to the reference viscosity, η_0, E_η is the dimensional activation energy (EUM in the upper mantle and ELM in the lower mantle), R is the universal gas constant, T is the temperature, T_η is a temperature offset, and T_b is the ambient mantle temperature outside the thermal lithosphere, slabs or the basal thermal boundary layer (see Table S1). The modelling parameters were set following ref. [38] to adapt properties of ambient mantle and lithosphere in East Asia.

Declarations

Data availability

The P wave tomography model UU-P07 is available at https://www.atlas-of-the-underworld.org/uu-p07-model/. MIT-P08 is from ref.[40]. The plate reconstruction model of ref.[22] and the GPlates software tool are available at www.gplates.org/. Other materials of this study are available upon request from the corresponding authors.

Author contributions

Y.H.S. contributed to the structural interpretation and analyses, and completed the original draft; H.D., D.D.P. and Y.C.L. jointly performed the geodynamic models; L.J.L. discussed the model results with Y.H.S and revised the manuscript; S.Z.L. funded this study and discussed the crustal structure with Y.H.S.; J.P.L. and X.Z.C. carried out the plate reconstructions; L.M.D. and X.Z.C. helped to writing the methods and the supporting information.

Acknowledgements

This study is funded by the Marine S&T Fund of Shandong Province for National Laboratory for Marine Science and Technology (Qingdao) (2022QNLM050302), National Natural Science Foundation of China (42121005, 91958214, 41876036), National Natural Science Foundation of Shandong Province (ZR2021YQ25) and Fundamental Research Funds for the Central Universities (202172003). Most figures are mapped with GMT (https://www.generic-mapping-tools.org/) and Paraview (https://www.paraview.org/).

References

1. Li, J. B., Ding, W. W., Lin, J., Xu, Y. G., Kong, F. S. & Li, S. Z. Dynamic processes of the curved subduction system in Southeast Asia: A review and future perspective. Earth-Science Reviews 217, 103647 (2020).
2. Zhou, D., Sun, Z., Chen, H. Z., Xu H. H., Wang W. Y., Pang, X., Cai, D. S. & Hu, D. K. Mesozoic paleogeography and tectonic evolution of South China Sea and adjacent areas in the context of Tethyan and Paleo-Pacific interconnections. Island Arc 17, 186–207 (2008).
3. Ding, W. W. Continental margin dynamics of South China Sea: From continental break-up to seafloor spreading. Earth Science 46(3), 790–800 (2021) (in Chinese with English abstract).
4. Li, S. Z., Suo, Y. H., Zhou, J., Wang, G. Z., Li, X. Y., Jiang, Z. X., Liu, J. P., Liu, L. J., Liu, Y. J., Zhan, H. W., Jiang, S. H., Cheng, H. H., Wang, P. C., Zhu, J. J., Dai, L. M., Dong, H., Liu, L. & Guo, X. Y. Tectonic Evolution of the South China Ocean-Continent Connection Zone: Transition and Mechanism of the Tethyan to the Pacific Tectonic Domains. Journal of Geomechanics 28(5), DOI: 10.12090/j.issn.1006-6616.20222809 (2022).
5. Lin J., Xu, Y., Sun, Z. & Zhou Z. Mantle upwelling beneath the South China Sea and links to surrounding subduction systems. National Science Review 6, 877–881 (2019).

6. Clift, P. D. & Lin, J. Preferential mantle lithospheric extension under the South China margin. Mar. Pet. Geol. 18 (8), 929–945 (2001).
7. Ding, W., Sun, Z., Mohn, G., Nirrengarten, M., Tugend, J., Manatschal, G. & Li, J. Lateral evolution of the rift-to-drift transition in the South China Sea: evidence from multichannel seismic data and IODP Expeditions 367&368 drilling results. Earth Planet. Sci. Lett. 531, 115932 (2020).
8. Larsen, H. C., Mohn, G., Nirrengarten, M., Sun, Z., Stock, J., Jian, Z., Klaus, A., Alvarez-Zarikian, C. A., Boaga, J., Bowden, S. A., Briais, A., Chen, Y., Cukur, D., Dadd, K., Ding, W., Dorais, M., Ferré, E. C., Ferreira, F., Furusawa, A., Gewecke, A., Hinojosa, J., Höfig, T. W., Hsiung, K. H., Huang, B., Huang, E., Huang, X. L., Jiang, S., Jin, H., Johnson, B. G., Kurzawski, R. M., Lei, C., Li, B., Li, L., Li, Y., Lin, J., Liu, C., Liu, C., Liu, Z., Luna, A. J., Lupi, C., McCarthy, A., Ningthoujam, L., Osono, N., Peate, D. W., Persaud, P., Qiu, N., Robinson, C., Satolli, S., Sauermilch, I., Schindlbeck, J. C., Skinner, S., Straub, S., Su, X., Su, C., Tian, L., van der Zwan, F. M., Wan, S., Wu, H., Xiang, R., Yadav, R., Yi, L., Yu, P. S., Zhang, C., Zhang, J., Zhang, Y., Zhao, N., Zhong, G. & Zhong, L. Rapid transition from continental breakup to igneous oceanic crust in the South China Sea. Nature Geoscience 11, 782–789 (2018).
9. Hilde, T. W. C., Uyeda, S. & Kroenke, L. Evolution of the western Pacific and its margin. Tectonophysics 38(1–2), 145–165 (1977).
10. Tapponnier, P., Peltzer, G., Ledain, A. Y., Armijo, R. & Cobbold, P. Propagating extrusion tectonics in Asia—new insights from simple experiments with plasticine. Geology 10(12), 611–616 (1982).
11. Briais, A., Patriat, P. & Tapponnier, P. Updated interpretation of magnetic-anomalies and sea-floor spreading stages in the South China Sea—implications for the tertiary tectonics of southeast-Asia. J. Geophys. Res. 98(B4), 6299–6328 (1993).
12. Holloway, N. H. North Palawan Block, Philippines—its relation to Asian Mainland and role in evolution of South China Sea. AAPG Bull 66(9), 1355–1383 (1982).
13. Taylor, B. & Hayes, D. E. Origin and history of the South China Sea basin, Part 2. In The tectonic and geologic evolution of Southeast Asian Seas and Islands. https://doi.org/10.1029/gm027p0023 (1983).
14. Hall, R. Reconstructing Cenozoic SE Asia. In: Hall R, Blundell DJ (eds) Tectonic evolution of southeast Asia, vol 106., Geol Soc Lond Spec Publ, London, pp 203–224 (1996).
15. Flower, M. F. J., Tamaki, K. & Hoang, N. Mantle extrusion: a model for dispersed volcanism and DUPAL-like asthenosphere in east Asia and the western Pacific. In: Flower MEJ, Chung SL, Lo C H (eds) Mantle dynamics and plate interactions in east Asia, vol 27. AGU, Geodynamics, pp 67–88 (1998).
16. Sun, Z., Lin, J., Qiu, N., Jian, Z. M., Wang, P. X., Pang, X., Zheng, J. Y. & Zhu, B. D. The Role of Magmatism in the Thinning and Breakup of the South China Sea Continental Margin. National Science Review 6(5), 871–876 (2019).
17. Cao, L., He, X., Zhao, L., Lü, C., Hao, T., Zhao, M. & Qiu, X. Mantle flow patterns beneath the junction of multiple subduction systems between the Pacific and Tethys domains, SE Asia: Constraints from

SKS-wave splitting measurements. Geochemistry, Geophysics, Geosystems, 22, e2021GC009700 (2021).

18. Wu, J., Suppe, J., Lu, R. & Kanda, R. Philippine Sea and East Asian plate tectonics since 52 Ma constrained by new subducted slab reconstruction methods. J. Geophys. Res. Solid Earth 121, 4670–4741 (2016).
19. Zhu, J., Li, S., Jia, Y., Zhang, S., Chen, X., Chen, R., Suo, Y., Cao, X., Jia, Z., Ou, X., Liu, J., Wang, P. & Zhou, J. Links of high velocity anomalies in the mantle to the Proto-South China Sea slabs: Tomography-based review and perspective. Earth-Science Reviews, 104074 (2022).
20. Shao, L., You, H., Hao, H., Wu, G., Qian, P. & Lei, Y. Petrology and depositional environments of Mesozoic strata in the northeastern South China Sea (in Chinese with English Abstract). Geological Review 53, 1–6 (2007).
21. Yan, P., Wang, L., & Wang, Y. Late Mesozoic compressional folds in Dongsha Waters, the northern margin of the South China Sea. Tectonophysics 615, 213–223 (2014).
22. Ye, Q., Mei, L., Shi, H., Camanni, G., Shu, Y., Wu, J., Yu, L., Deng, P. & Li, G. The late cretaceous tectonic evolution of the South China Sea area: An overview, and new perspectives from 3D seismic reflection data. Earth-Science Reviews 187, 186–204 (2018).
23. Deng, H., Ren, J., Pang, X., Rey, P. F., McClay, K. R., Watkinson, I. M., Zheng, J. Y. & Luo, P. South China Sea Documents the Transition from Wide Continental Rift to Continental Break Up. Nature Communications 11(1), 4583 (2020).
24. Ru, K. & Pigott, J. D. Episodic rifting and subsidence in the South China Sea. American Association of Petroleum Geologists Bulletin 70, 1136–1155(1986).
25. Müller, R. D., Seton, M., Zahirovic, S., Williams, S. E., Matthews, K. J., Wright, N. M., Shephard, G., Maloney, K. T., Barnett-Moore, N., Hosseinpour, M., Bower, D. J. & Cannon, J. Ocean basin evolution and global-scale plate reorganization events since Pangea breakup. Annu. Rev. Earth Planet. Sci. 44 (2016).
26. Liu, J. P., Li, S. Z., Cao, X. Z., Dong, H., Suo, Y. H., Jiang, Z. X., Zhou, J., Li, X. Y., Zhang, R. X., Liu, L. J. & Foulger, G. R. Back-arc tectonic response to mantle micro-block deep processes as revealed by reconstruction of the Philippine Sea-South China Sea region since the Eocene. *Under review by Geophysical Research Letters* (2022).
27. Suo, Y. H., Li, S. Z., Peng, G. R., Du, X. D., Zhou, J., Wang, P. C., Wang, G. Z., Somerville, I., Diao, Y. X., Liu, Z. Q., Fu, X. J., Liu, B. & Cao, X. Z. Cenozoic basement-involved rifting of the northern South China Sea margin. Gondwana Research, https://doi.org/10.1016/j.gr.2022.02.017 (2022).
28. Ye, Q., Mei, L., Shi, H., Du, J., Deng, P., Shu, Y. & Camanni, G. The influence of pre-existing basement faults on the Cenozoic structure and evolution of the proximal domain, northern South China Sea rifted margin. Tectonics 39, e2019TC005845 (2020).
29. Pang, X., Ren, J., Zheng, J., Liu, J., Peng, Y. & Liu, B. Petroleum geology controlled by extensive detachment thinning of continental margin crust: a case study of Baiyun sag in the deep-water area of northern South China Sea. Pet. Explor. Dev. 45, 29–42 (2018).

30. Buck, W. R. Modes of Continental Lithospheric Extension. J. Geophys. Res. 96, 20161–20178 (1991).
31. England, C. Constraints on extension of continental lithosphere. J. Geophys. Res. 88, 1145–1152 (1983).
32. Zhang, C., Manatschal, G., Pang, X., Sun, Z., Zheng, J., Li, H., Sun, L., Zhang, J. & Zhao, Y. Discovery of mega-sheath folds flooring the Liwan subbasin (South China Sea): Implications for the rheology of hyperextended crust. Geochemistry, Geophysics, Geosystems, 21, e2020GC009023 (2020).
33. Li, C. F., Xu, X., Lin, J., Sun, Z., Zhu, J., Yao, Y. J., Zhao, X. X., Liu, Q. S., Kulhanek, D. K., Wang, J., Song, T. R., Zhao, J. F., Qiu, N., Guan, Y. X., Zhou, Z. Y., Williams, T., Bao, R., Briais, A., Brown, E. A., Chen, Y. F., Clift, P. D., Colwell, F. S., Dadd, K. A., Ding, W. W., Almeida, I. H., Huang, X. L., Hyun, S. M., Jiang, T., Koppers, A. A. P., Li, Q. Y., Liu, C. L., Liu, Z. F., Nagai, R. H., Peleo-Alampay, A., Su, X., Tejada, M. L. G., Trinh, H. S., Yeh, Y. C., Zhang, C. L., Zhang, F. & Zhang, G. L. Ages and magnetic structures of the South China Sea constrained by deep tow magnetic surveys and IODP Expedition 349. Geochem. Geophys. Geosyst. 15, 4958–4983 (2014).
34. Ding, W. & Li, J. Propagated rifting in the southwest sub-basin, South China Sea: insights from analogue modelling. J. Geodyn. 17, 71–86 (2016).
35. Barckhausen, U., Engels, M., Franke, D., Ladage, S. & Pubellier, M. Evolution of the South China Sea: revised ages for breakup and seafloor spreading. Mar. Petrol. Geol., 10.1016/j.marpetgeo.2014.02.022 (2014).
36. Liu, Y. M., Liu, L. J., Li, Y.C., Peng, D. D., Wu, Z. P., Cao, Z. B., Li, S. Z. & Du, Q. Z. Global back-arc extension due to trench-parallel mid-ocean ridge subduction. To be published in Earth Planetary Science Letters 600, 1178889(2022).
37. Hu, J. S., Liu, L. J. & Zhou, Q. Reproducing past subduction and mantle flow using high-resolution global convection models. Earth and Planetary Physics 2(3), 189–207 (2018).
38. Peng, D., Liu, L., Hu, J., Li, S., & Liu, Y. Formation of East Asian stagnant slabs due to a pressure-driven Cenozoic mantle wind following Mesozoic subduction. Geophysical Research Letters 48, e2021GL094638 (2021).
39. Amaru, M. Global travel time tomography with 3-D reference models. Geologica Ultraiectina (2007).
40. Li, C., Van Der Hilst, R. D., Engdahl, E. R. & Burdick, S. A new global model for P wave speed variations in Earth's mantle. Geochemistry Geophys. Geosystems 9, https://doi.org/10.1029/2007GC001806 (2008).
41. Peng, D., Liu, L., & Wang, Y. A newly discovered Late-Cretaceous East Asian flat slab explains its unique lithospheric structure and tectonics. Journal of Geophysical Research: Solid Earth 126, e2021JB022103 (2021).
42. Liu, L. & Stegman, D. R. Segmentation of the Farallon slab. Earth and Planetary Science Letters 311(1–2), 1–10 (2011).
43. Schellart, W. P., Stegman, D. R., Farrington, R. J., Freeman, J. & Moresi, L. Cenozoic Tectonics of Western North America Controlled by Evolving Width of Farallon Slab. Science 329, 316–319 (2010).

44. Huang, C.-Y., Wang, P. X., Yu, M. M., You, C.-F., Liu, C.-S., Zhao, X. X., Shao, L., Zhong, G. F. & Yumul, G. P. Jr. Potential role of strike-slip faults in the opening up of the South China Sea. National Science Review 6(5), 891–901 (2019).
45. Liu, L., Peng, D., Liu, L., Chen, L., Li, S., Wang, Y., Cao, Z. & Feng, M. East Asian lithospheric evolution dictated by multistage Mesozoic flat-slab subduction. Earth-Science Reviews 217, 103621 (2021).
46. Hall, R. & Breitfeld, H. T. Nature and demise of the Proto-South China Sea. Bull. Geol. Soc. Malaysia 63, 61–76 (2017).
47. Cullen, A. Nature and significance of the West Baram and Tinjar Lines, NW Borneo. Marine and Petroleum Geology 51, 197–209 (2014).
48. Ren, J., Tamaki, K., Li, S. & Zhang, J. X. Late Mesozoic and Cenozoic rifting and its dynamic setting in Eastern China and adjacent areas. Tectonophysics 344(3–4), 175–205 (2002).
49. Suo, Y. H., Li, S. Z., Yu, S., Somerville, I. D., Liu, X., Zhao, S. J. & Dai, L. M. Cenozoic tectonic jumping and implications for hydrocarbon accumulation in basins in the East Asia Continental Margin. Journal of Asian Earth Sciences 88, 28–40 (2014).
50. Hall, R. & Spakman, W. Mantle structure and tectonic history of SE Asia. Tectonophysics 658, 14–45 (2015).
51. Hutchison, C. S. Geological Evolution of South-East Asia. Oxford Clarendon Press (1989).
52. Lee, T.-Y. & Lawer, L. A. Cenozoic plate reconstruction of Southeast Asia. Tectonophysics 251, 85–138 (1995).
53. Gatinsky, Y. G. & Hutchison, C. S. Cathaysia, Gondwanaland and the Paleotethys in the evolution of continental Southeast Asia. Bulletin of the Geological Society of Malaysia 20, 179–199 (1986).
54. Liu, L., Gurnis, M., Seton, M., Saleeby, J., Müller, R. D. & Jackson, J. M. The role of oceanic plateau subduction in the Laramide orogeny. Nature Geoscience 3(5), 353–357 (2010).
55. Ye, Y. C. et al. Chapter 4 - Active Faults of Sea Area, Editor(s): Ye Yincan et al, Marine Geo-Hazards in China, Elsevier, Pages 89-128, ISBN 9780128127261, https://doi.org/10.1016/B978-0-12-812726-1.00004-8 (2017).
56. Chai, L. G. The nature of Yushan-Kume Fault Belt and its control over East China Sea. Oil & Gas Geology 7(2), 107–115 (1986) (in Chines with English abstract).
57. Koptev, A., Calais, E., Burov, E., Leroy, S. & Gerya, T. Along-axis transition between narrow and wide rifts: Insights from 3D numerical experiments. Geophysical Research Abstracts Vol. 18, EGU2016-6511, EGU General Assembly 2016 (2016).
58. Li, F., Sun, Z. & Yang, H. Possible spatial distribution of the Mesozoic volcanic arc in the present-day South China Sea continental margin and its tectonic implications. Journal of Geophysical Research: Solid Earth 123, 6215–6235 (2018).
59. Yan, P., Deng, H., Liu, H., Zhang, Z. & Jiang, Y. The temporal and spatial distribution of volcanism in the South China Sea region. J. Asian Earth Sci. 27, 647–659 (2006).

60. Zhang, G. L., Luo, Q., Zhao, J., Jackson, M. G., Guo, L. S. & Zhong, L. F. Geochemical nature of sub-ridge mantle and opening dynamics of the South China Sea. Earth Planet. Sci. Lett. 489, 145–155 (2018).
61. Briais, A., Tapponnier, P. & Pautot, G. Constraints of Sea Beam data on crustal fabrics and seafloor spreading in the South China Sea. Earth and Planetary Science Letters 95(3–4), 307–320 (1989).
62. Leloup, P. H., Harrison, T. M., Ryerson, F. J., Chen, W.J., Li, Q., Tapponnier, P. & Lacassin, R. Structural, petrological and thermal evolution of a Tertiary ductile strike-slip shear zone, Diancang Shan, Yunnan. J. Geophys. Res. 98(B4), 6715–6743(1993).
63. Jolivet, M., Brunel, M., Seward, D., Xu, Z., Yang, J., Roger, F., Tapponnier, P., Malavieille, J., Arnaud, N. & Wu, C. Mesozoic and Cenozoic tectonics of the northern edge of the Tibetan plateau: fission-track constraints Tectonophysics 343 (1–2), 111–134 (2001).
64. Sibuet, J. C., Yeh, Y. C. & Lee, C. S. Tectonophysics geodynamics of the South China Sea. Tectonophysics 692, 98–119 (2016).
65. Liu, W., Gai, C., Feng, W., Cao, W., Guo, L., Zhong, Y., et al. Coeval evolution of the Eastern Philippine Sea Plate and the South China Sea in the Early Miocene: Paleomagnetic and provenance constraints from ODP Site 1177. Geophysical Research Letters 48, e2021GL093916 (2021).
66. Wang, P., Li, S., Guo, L., Zhao, S., Li, X., Wang, Y., Hui, G. & Wang, Q. Opening of the South China Sea (SCS): a joint effect of dextral strike-slip pull-apart and proto-SCS slab pull. Earth Sci. Front. 24, 294–319 (2017).
67. Jolivet, L. Japan Sea, opening history and mechanism: A synthesis. Journal of Geophysical Research 99, 22237–22259 (1994).
68. Xu, J. Y., Ben-Avraham, Z., Kelty, T., & Yu, H. S. Origin of marginal basins of the NW Pacific and their plate tectonic reconstructions. Earth-Science Reviews 130, 154–196 (2014).
69. Zhong, S., McNamara, A., Tan, E., Moresi, L. & Gurnis, M. A benchmark study on mantle convection in a 3-D spherical shell using CitcomS. Geochemistry, Geophys. Geosystems 9, 1–32 (2008).
70. Hu, J., Liu, L., Zhou, Q. & Zhou, Q. Reproducing past subduction and mantle flow using high-resolution global convection models. Earth and Planetary Physics 2(3), 189–207 (2018).

Figures

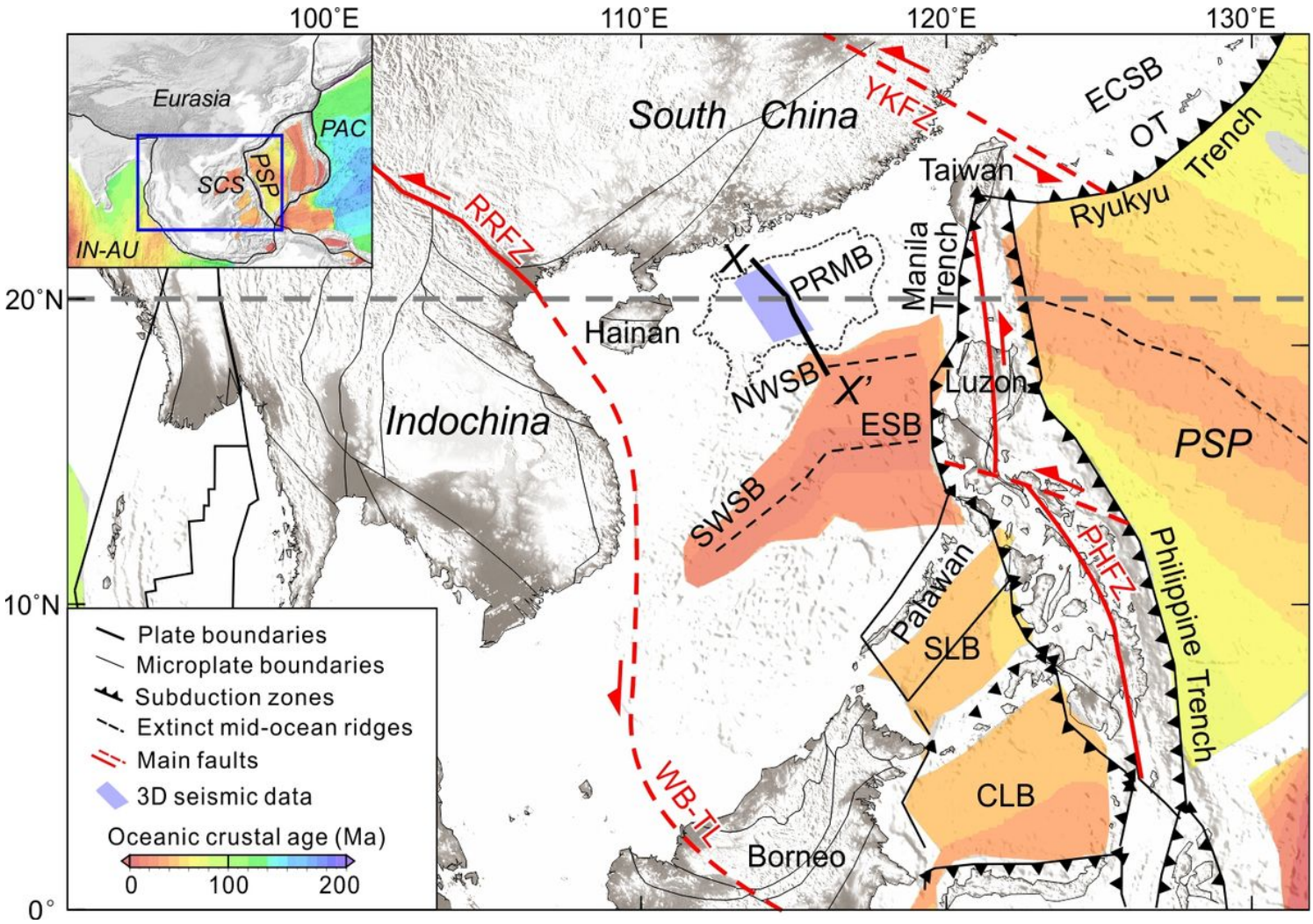

Figure 1

Location of the SCS at the convergent zone of the Eurasian, Philippine Sea and Indian-Australian plates. *Grey dashed lines mark the position of the cross-section (along 20°N) shown in Fig. 3. Abbreviations: CLB- Celebes Basin, ECSB- East China Sea Shelf Basin, ESB- East Subbasin, NWSB- Northwest Subbasin, PRMB- Pearl River Mouth Basin, SLB- Sulu Basin, SWSB- Southwest Subbasin, OT- Okinawa Trough, IN-AU– Indian-Australian Plate, PSP- Philippine Sea Plate, PHFZ- Philippine Fault Zone, RRFZ- Red River Fault Zone, WB-TL– West Baram- Tinjar Line, YKFZ- Yushan-Kume Fault Zone.*

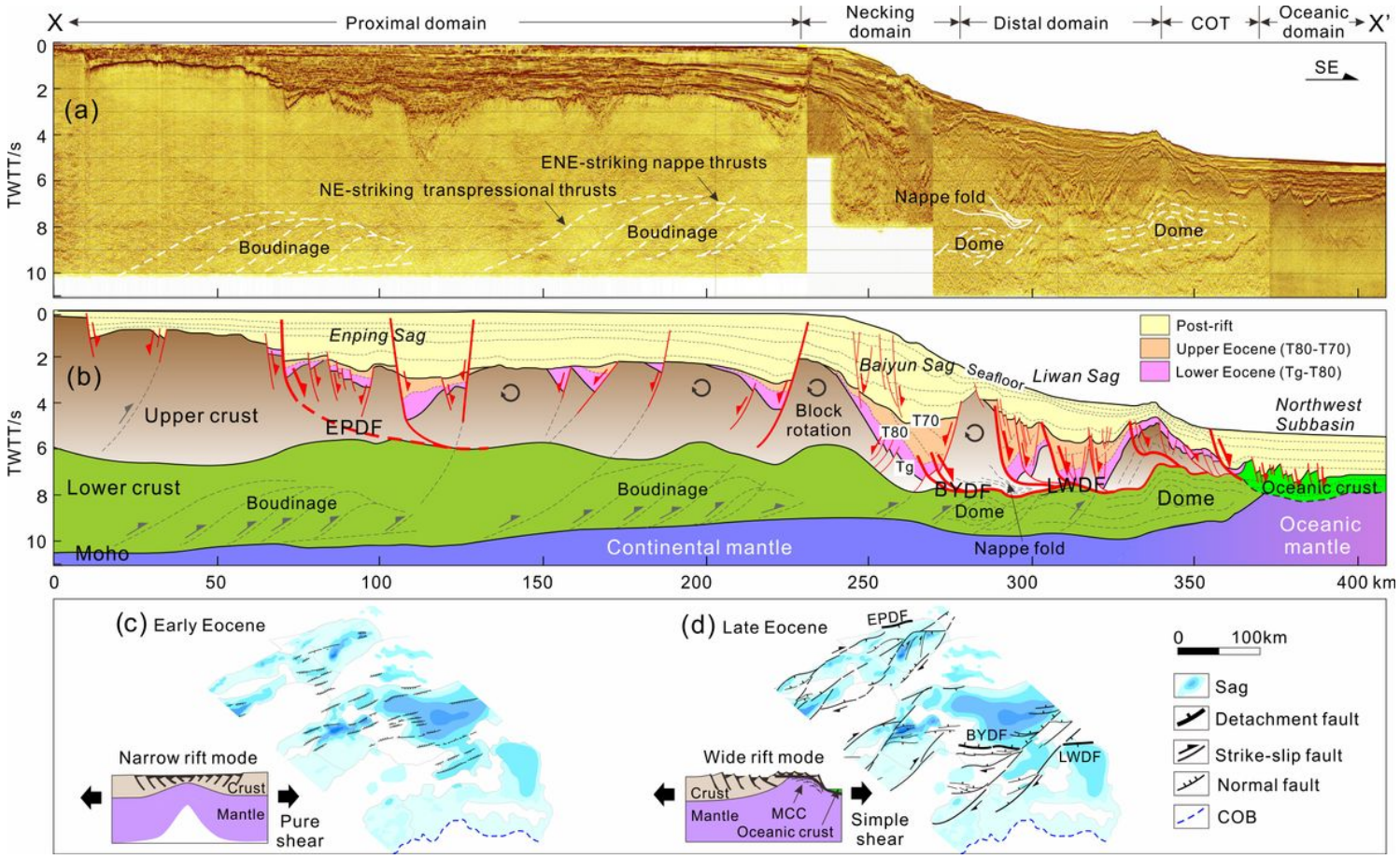

Figure 2

Syn-rift crustal structure of the PRMB. *(a-b) Seismic interpretation of profile X–X' (marked as black solid line in Fig. 1) shows the two-phase syn-rift structures. The upper crust consists of a nappe fold within the titled block between the Baiyun Sag and Liwan Sag[7]. The lower crust develops a series of boudinage or dome structures[7, 27-28, 32], constituted by the ENE-striking nappe thrusts and the NE-striking transpressional faults[27]. (c-d) Map view of the two-phase syn-rifting structures in the 3D seismic area (the blue polygon in Fig. 1) and the corresponding rift modes. Rift modes were revised from ref.[31]. The Early Eocene syn-rift unit is composed by a series of grabens, controlled by the localized ENE-striking normal faults. The Late Eocene syn-rift unit is characterized by the seaward dipping detachment faults and a rhomb-shaped architecture. Abbreviations: BYDF- Baiyun Detachment Fault, EPDF- Enping Detachment Fault, LWDF- Liwan Detachment Fault, COB- Continent ocean boundary, COT- Continent ocean transition zone, MCC- Metamorphic core complex.*

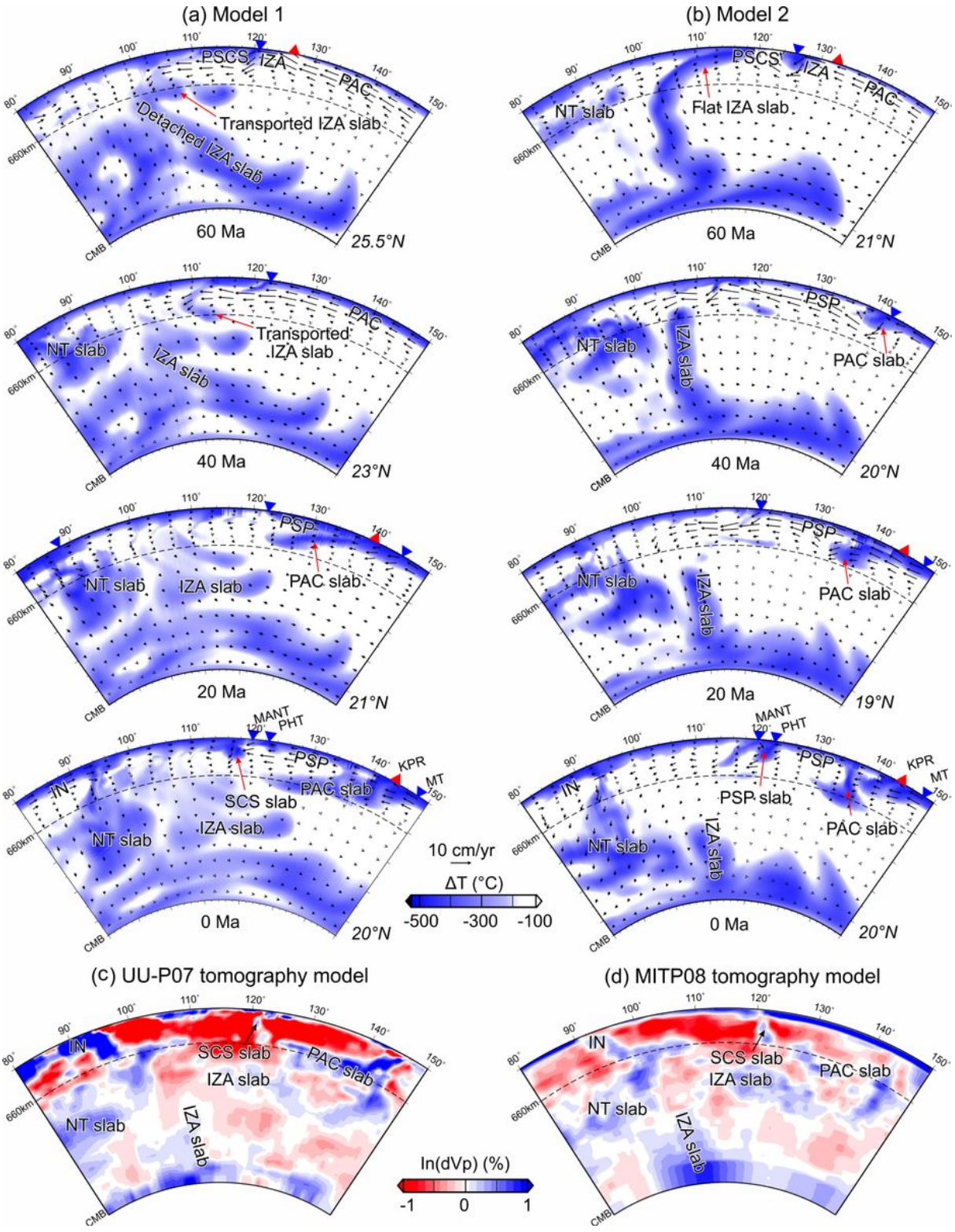

Figure 3

Comparison of seismic tomography with predicted temperature field along E-W profiles across the PRMB. *(a-b) Evolution of the modeled mantle flows in Model 1 and in Model 2. The profile location was fixed along 20°N since 60 Ma in Model 2, due to a moving hotspot reference frame that positions the PRMB around this latitude in ref.[25]. In Model 1, tracking the location of PRMB requires shifting the profile from 25.5°N at 60 Ma southward to 23°N at 40 Ma and then to 20°N till the present, because the adopted plate*

reconstruction in ref.[26] was based on an optimized mantle reference frame (Fig. S1). Blue triangles show the trench positions. Red triangles show the mid-ocean ridge locations. (c-d) Seismic tomography along 20°N from UU-P07[39] and MITP08[40]. Abbreviations: CMB- Core mantle boundary, KPR-Kyushu-Palau Ridge, MANT- Manila Trench, MT- Mariana Trench, PHT- Philippine Trench; IN- Indian Plate; NT- Neo-Tethys Ocean.

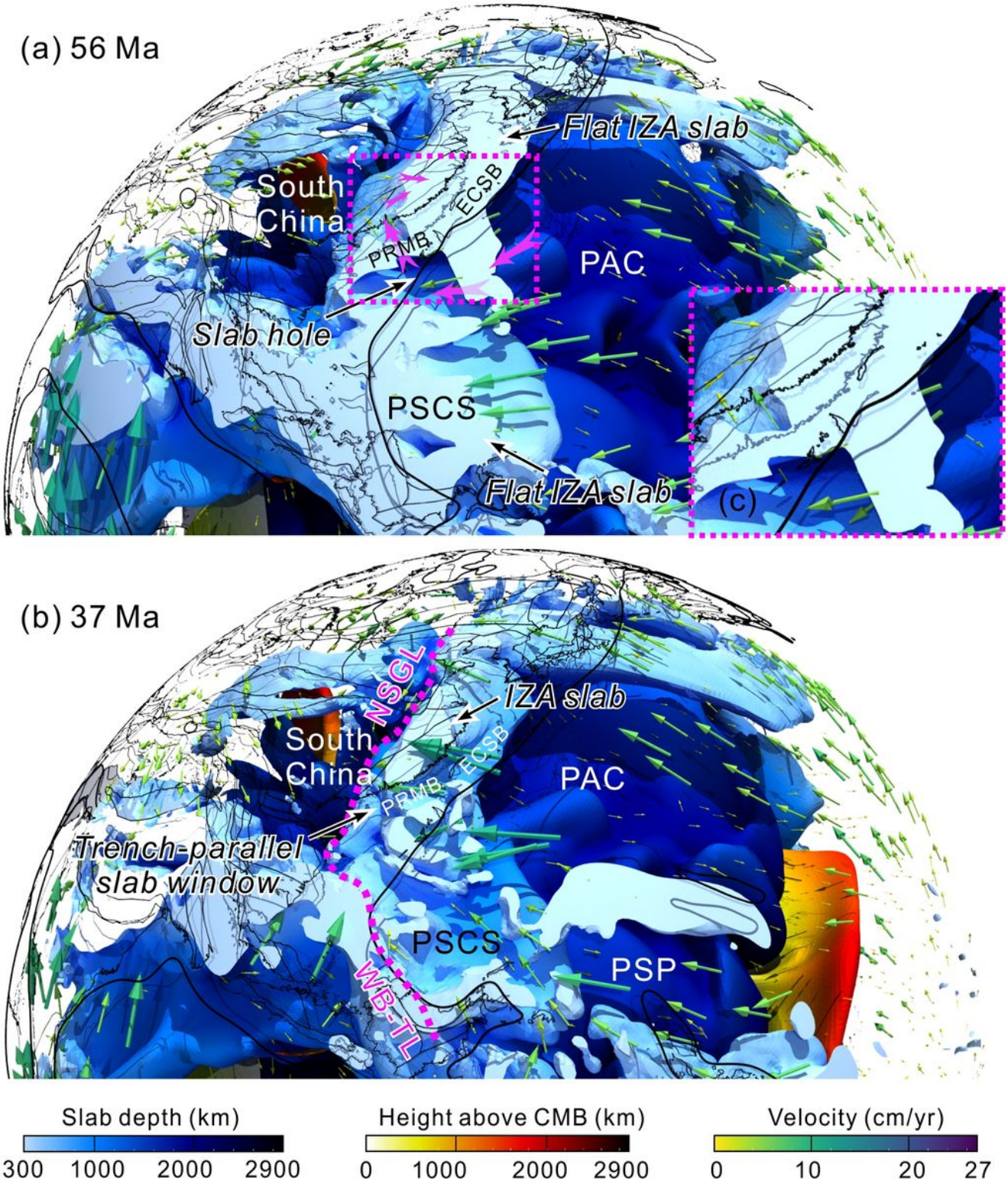

Figure 4

3D view of the modelled slabs and mantle velocities at 56 Ma (a) and 37 Ma (b) in Model 1. *Slabs colored by depth (> 300km) are represented as isovolumes with non-dimensional temperature lower than 0.45. Thick black solid lines mark the location of COB. At 56 Ma, the purple arrows schematically show the regional toroidal mantle flow around the slab edge, with an enlarged view in figure (c). The Tethyan tectonic domain from the west may get evolved into the toroidal mantle flow. A clear boundary between the Pacific and Tethyan tectonic domains has not formed yet. At 37 Ma, the slab hole grew into the broad trench-parallel slab window under East Asian margin. The broad slab window allowed the voluminous asthenosphere from the Pacific Plate side to pour into the mantle wedge under East Asia, giving rise to the strong landward mantle wind. A boundary separating the Pacific tectonic domain and the Tethyan tectonic domain occurred along the North-South Gravity Lineament (NSGL) in East Asia[45] and the West Baram-Tinjar Line (WB-TL) in Southeast Asia[46], roughly marked by the dotted magenta line.*

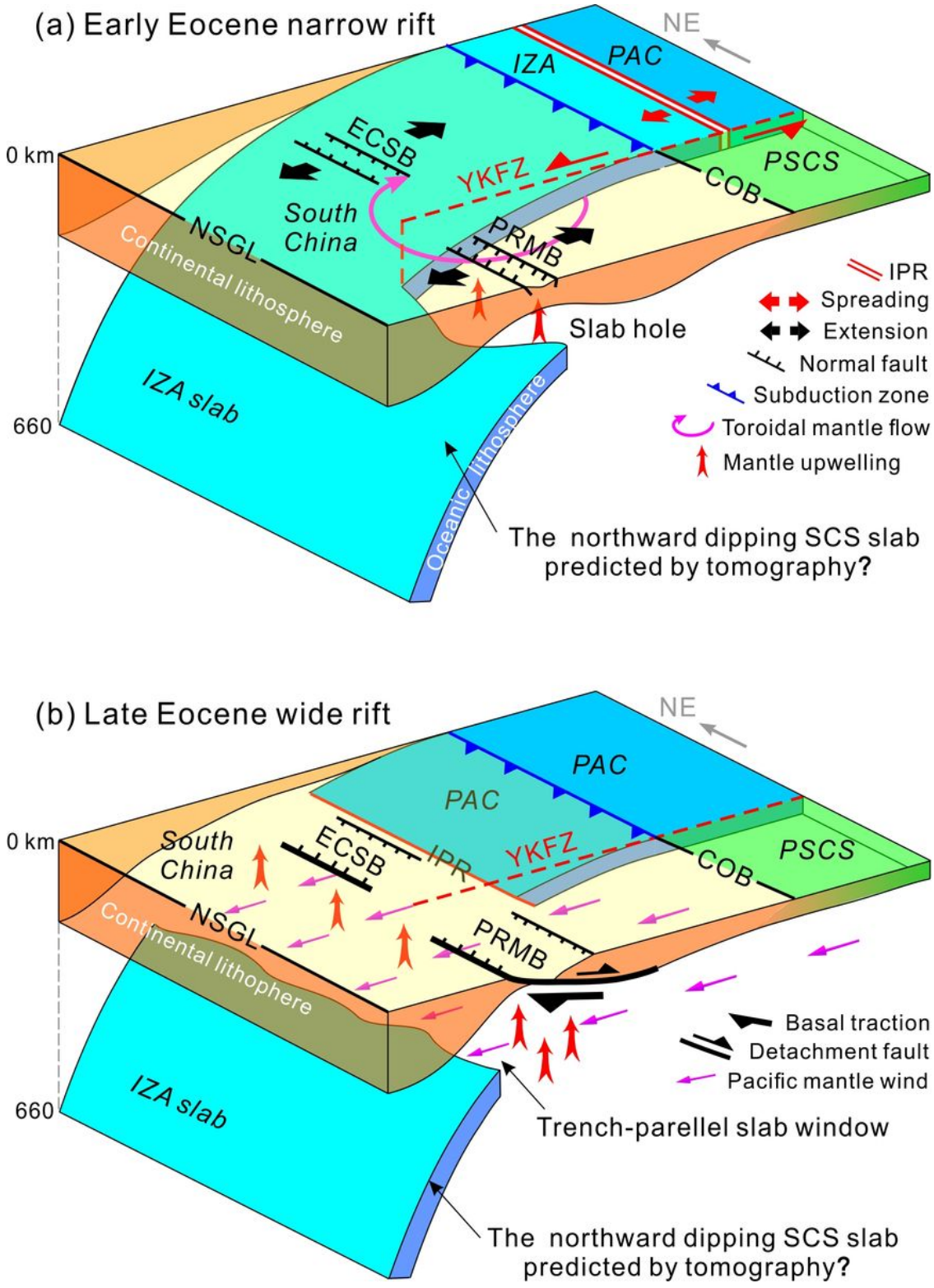

Figure 5

3D sketch showing the two-phase continental rifting dominated by the mantle flow associated with the Pacific subduction system. *(a) During the Early Eocene, the toroidal mantle flow around the slab edge that was torn by the NW-trending transform plate boundary triggered the narrow rifting of the PRMB and the ECSB. The associated slab hole allowed less amount of mantle upwelling, attributed to a weakly stretched lithosphere. (b) During the Late Eocene, the toroidal mantle flow was replaced by the strong*

landward mantle wind, when the slab hole grew into the broad trench-parallel slab window associated with the subduction of the Izanagi-Pacific mid-ocean ridge (IPR). The mantle wind exerted stronger landward basal traction on the South China continental lithosphere to the east of the North-South Gravity Lineament (NSGL), stretching the narrow rift into the wide rift characterized by seaward dipping detachment faults. The broad trench-parallel slab window allowed fertile mantle upwelling. So, the northern SCS margin also transitioned from magma-poor to magma-rich, representing an intermediate rifted margin with features from both traditional end-member extremes.

Supplementary Files

This is a list of supplementary files associated with this preprint. Click to download.

- SubmitedtoNGSupportingfile.docx